ANALOG DEVICES

AN-1386
APPLICATION NOTE

One Technology Way • P.O. Box 9106 • Norwood, MA 02062-9106, U.S.A. • Tel: 781.329.4700 • Fax: 781.461.3113 • www.analog.com

The Effects of the Sample Clock Spectrum on Measured Signal Spectrum in ADCs, a Simple Mathematical Description

by Benjamin Babjak

INTRODUCTION

The performance of contemporary high speed analog-to-digital converters (ADCs) depends directly on their clocks. However, the oscillators in the signal generators employed to generate these clocks are nonideal; both clock amplitude and phase may deviate from the ideal. The ADC sampling circuits tend to be resilient to small clock amplitude changes; however, even small phase offsets can have a profound effect on the ADC output. Therefore, the phase noise of clock oscillators must be carefully examined if accurate readings are to be taken with high speed ADCs.

This application note provides an overview of the well established but, in practice, fairly unused mathematical background necessary to understand the effects of the clock and analog input phase noise. It discusses the differences and similarities between amplitude noise and phase noise, suggests simple formulas to estimate the sideband power, and clarifies the mechanisms that couple clock and analog input noise onto measured ADC signals.

Finally, it also shows how these methods can be applied for contemporary high speed ADC evaluation and performance estimation, using the AD9684 as an example.

TABLE OF CONTENTS

REVISION HISTORY

6/2016—Revision 0: Initial Version

AMPLITUDE NOISE vs. PHASE NOISE

Sinusoidal waves are the predominant clock waveforms for high speed ADCs because they are easier to generate, transfer, and match at RF frequencies than other waveforms, such as square waves. Sinusoidal waves can be described mathematically as follows:

$$c(t) = A_c \sin\omega_c t$$

where:
$c(t)$ is the carrier (clock).
A_c is the carrier amplitude.
ω_c is the angular frequency.
t is time.

Typically, clock signals are high power (that is, >13 dBm), which alleviates losses in the cabling, connectors, and traces. It can be safely assumed that the clock power is higher than noise power.

APPROXIMATING TRIGONOMETRIC FUNCTIONS

The following approximations for x << 1 are used extensively throughout this application note. Therefore, it is important to be aware when these approaches break down, and what happens after. These simple, linear approximations produce increasing error for larger x values, as shown in Figure 1.

$$\sin(x) = \sum_{k=0}^{\infty} \frac{(-1)^k x^{1+2k}}{(1+2k)!} = x - \frac{x^3}{3!} + \frac{x^5}{5!} - \frac{x^7}{7!} + \cdots \approx x$$

$$\cos(x) = \sum_{k=0}^{\infty} \frac{(-1)^k x^{2k}}{(2k)!} = 1 - \frac{x^2}{2!} + \frac{x^4}{4!} - \frac{x^6}{6!} + \cdots \approx 1$$

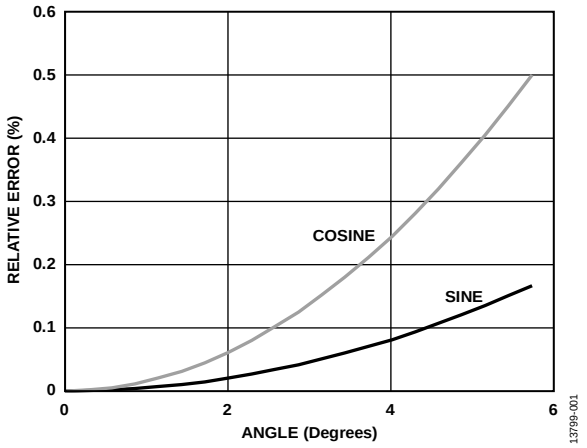

Figure 1. Approximation Error for Trigonometric Functions

DETERMINISTIC APPROACH

The first subject is clock noise, which is assumed to be sinusoidal in the following proof. This simplification allows examination of the phase between the carrier and the noise. Amplitude noise is discussed as a form of amplitude modulation (AM).

$$\begin{aligned} c_{AM}(t) &= (1 - A_n \cos\omega_n t) A_c \sin\omega_c t \\ &= A_c \sin\omega_c t - A_c A_n \cos\omega_n t \sin\omega_c t \\ &= A_c \sin\omega_c t - \frac{A_c A_n}{2}\left(\sin(\omega_c + \omega_n)t + \sin(\omega_c - \omega_n)t\right) \end{aligned}$$

where:
$c_{AM}(t)$ is the carrier (clock) with AM noise.
A_c is the carrier amplitude.
A_n is the noise amplitude.
ω_n is the noise angular frequency.

Notice that AM generates two components: one below the carrier frequency and one above it. Therefore, this modulation is commonly referred to as double sideband (DSB). The phase of these two components are also aligned with the phase of the carrier; all of them are sines.

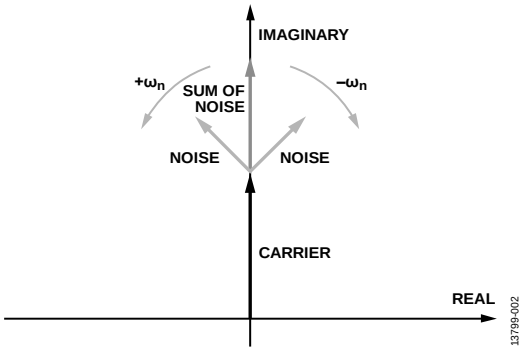

Figure 2. Phasor Diagram of an AM-DSB Modulated Signal

The phasor diagram of the signal in Figure 2 reveals the phase connection more intuitively. The sinω_ct carrier is depicted at a phase of 90° pointing vertically up. Compared to the carrier as reference, the two noise components rotate in opposing directions at an angular speed of ω_n. Their sum is therefore always a vector that falls in line with the carrier. In other words, the amplitude noise is always in phase with the carrier. Figure 3 shows the spectrum of such an AM modulated signal.

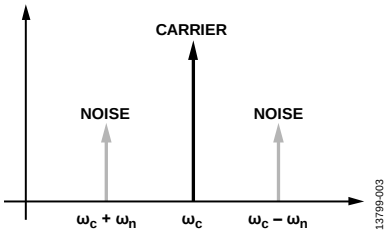

Figure 3. Spectrum of an AM-DSB Modulated Signal

The next subject is phase noise as a form of phase modulation (PM).

$$c_{PM}(t) = A_c \sin(\omega_c t + A_n \cos\omega_n t)$$
$$= A_c \sin\omega_c t \cos(A_n \cos\omega_n t) + A_c \cos\omega_c t \sin(A_n \cos\omega_n t)$$

A_n can be referred to as the phase modulation index in this context. If $A_n << 1$,

$$\cos(A_n \cos\omega_n t) \approx 1$$

$$\sin(A_n \cos\omega_n t) \approx A_n \cos\omega_n t$$

This allows the PM equation to be simplified:

$$c_{PM}(t) \approx A_c \sin\omega_c t + A_c A_n \cos\omega_c t \cos\omega_n t$$
$$= A_c \sin\omega_c t + \frac{A_c A_n}{2}\left(\cos\left(\omega_c + \omega_n\right)t + \cos\left(\omega_c - \omega_n\right)t\right)$$

Two noise components are found at the same frequencies as the AM-DSB case. The only difference is their phase, which is 90° off compared to the AM-DSB signal. Therefore, their sum is always perpendicular to the carrier. The phasor diagram and the signal spectrum help to visualize the signal (see Figure 4 and Figure 5).

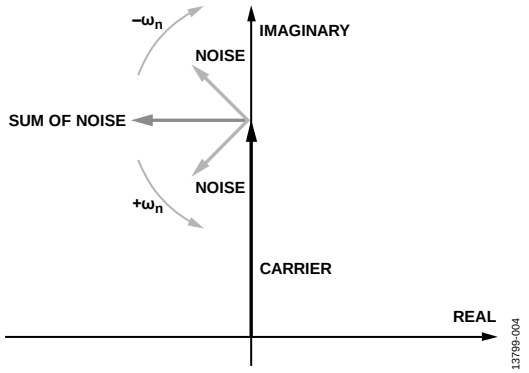

Figure 4. Phasor Diagram of a Low Modulation Index PM Signal

The figures also show one inherent problem of spectral analysis: the spectrum of an AM-DSB and a low modulation index PM signal are indistinguishable. Often AM and PM noise are simultaneously present, and the measured spectrum is a combination of their respective spectra.

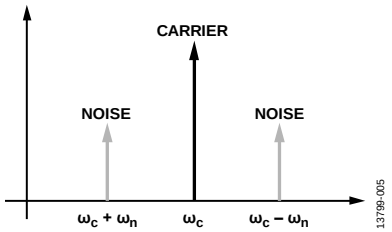

Figure 5. Spectrum of a Low Modulation Index PM Signal

STOCHASTIC APPROACH

Noise is not deterministic, nor is it sinusoidal in most cases. Therefore, the next topic of analysis is power spectral density (PSD) of stochastic noise. The spectrum includes negative frequencies, which correspond to the convention of how signals are analyzed in telecommunications.

It is assumed that the noise function, n(t), has an expected value of zero, that is, E[n(t)] = 0, and it has a DSB PSD of ν(ω), that is, ν(ω) = ν(−ω).

Starting with the AM noise signal,

$$c_{AM}(t) = (1 + n(t))A_c \sin\omega_c t$$

If its Fourier transform is defined as

$$\mathcal{F}\{c_{AM}(t)\} = C_{AM}(\omega) = \lim_{T\to\infty} \int_{-\frac{T}{2}}^{\frac{T}{2}} c_{AM}(t) e^{-j\omega t} dt$$

where T is the period time.

Then, the equations for its PSD can be written as follows:

$$PSD\{c_{AM}(t)\} = \gamma_{AM}(\omega) = \lim_{T\to\infty} \frac{1}{T} E\left[\left|C_{AM}(\omega)\right|^2\right]$$
$$= \lim_{T\to\infty} \frac{1}{T} E\left[\int_{-\frac{T}{2}}^{\frac{T}{2}} c_{AM}(t_1) e^{-j\omega t_1} dt_1 \int_{-\frac{T}{2}}^{\frac{T}{2}} c_{AM}(t_2) e^{j\omega t_2} dt_2\right]$$
$$= \lim_{T\to\infty} \frac{1}{T} \int_{-\frac{T}{2}}^{\frac{T}{2}} \int_{-\frac{T}{2}}^{\frac{T}{2}} E\left[c_{AM}(t_1) c_{AM}(t_2)\right] e^{-j\omega(t_1 - t_2)} dt_1 dt_2$$

The critical portion is the expected value expression within the integral; it is dealt with separately.

$$E[c_{AM}(t_1)c_{AM}(t_2)]$$
$$= E[(1 + n(t_1))A_c \sin\omega_c t_1 (1 + n(t_2))A_c \sin\omega_c t_2]$$
$$= A_c^2 \sin\omega_c t_1 \sin\omega_c t_2 E[(1 + n(t_1))(1 + n(t_2))]$$
$$= A_c^2 \sin\omega_c t_1 \sin\omega_c t_2 E[1 + n(t_1) + n(t_2) + n(t_1)n(t_2)]$$
$$= A_c^2 \sin\omega_c t_1 \sin\omega_c t_2 (1 + 0 + 0 + E[n(t_1)n(t_2)])$$
$$= \frac{A_c^2}{2}\left(\cos\omega_c\left(t_1 - t_2\right) - \cos\omega_c\left(t_1 + t_2\right)\right)\left(1 + E\left[n(t_1)n(t_2)\right]\right)$$

The t_1 and t_2 variables are replaced with $\tau = t_1 - t_2$ and $\upsilon = t_1 + t_2$. It is assumed that $E[n(t_1)n(t_2)]$ only depends on the time differences; therefore, it can be replaced with the autocorrelation, R(τ).

$$E\left[c_{AM}(t_1)c_{AM}(t_2)\right] = \frac{A_c^2}{2}\left(\cos\omega_c\tau - \cos\omega_c\upsilon\right)\left(1 + R(\tau)\right)$$

This result can be substituted back into the PSD calculation. The rules for changing variables in multiple integrals require the expression to be multiplied with the determinant of the Jacobian matrix, which is 1/2 in this case. Note that the variable change also affects the integration limits.

$$\gamma_{AM}(\omega) =$$
$$\frac{A_c^2}{4} \lim_{T\to\infty} \frac{1}{T} \int_{-T}^{T} \int_{-T+\tau}^{T+\tau} \left(\cos\omega_c\tau - \cos\omega_c\upsilon\right)\left(1 + R(\tau)\right) e^{-j\omega\tau} d\upsilon d\tau$$

Only ($\cos\omega_c\tau - \cos\omega_c\upsilon$) depends on the variable υ; therefore, it can be integrated separately.

$$\int_{-T+\tau}^{T+\tau}\left(\cos\omega_c\tau - \cos\omega_c\upsilon\right)d\upsilon = \cos\omega_c\tau\int_{-T+\tau}^{T+\tau}1\,d\upsilon - \int_{-T+\tau}^{T+\tau}\cos\omega_c\upsilon\,d\upsilon$$

$$= 2T\cos\omega_c\tau - \left[\frac{\sin\omega_c}{\omega_c}\right]_{-T+\tau}^{T+\tau}$$

$$= 2T\cos\omega_c\tau - 2\frac{\sin T\omega_c}{\omega_c}\cos\omega_c\tau$$

$$= 2T\cos\omega_c\tau\left(1-\frac{\sin T\omega_c}{T\omega_c}\right)$$

This further simplifies the PSD expression.

$$\gamma_{AM}(\omega) = \frac{A_c^2}{2}\lim_{T\to\infty}\left(1-\frac{\sin T\omega_c}{T\omega_c}\right)\int_{-T}^{T}\cos\omega_c\tau\left(1+R(\tau)\right)e^{-j\omega\tau}d\tau$$

$$= \frac{A_c^2}{2}\int_{-\infty}^{\infty}\cos\omega_c\tau\left(1+R(\tau)\right)e^{-j\omega\tau}d\tau$$

$$= \frac{A_c^2}{4}\int_{-\infty}^{\infty}\left(e^{j\omega_c\tau}+e^{-j\omega_c\tau}\right)\left(1+R(\tau)\right)e^{-j\omega\tau}d\tau$$

$$= \frac{A_c^2}{4}\int_{-\infty}^{\infty}e^{-j(\omega-\omega_c)\tau}d\tau + \frac{A_c^2}{4}\int_{-\infty}^{\infty}e^{-j(\omega+\omega_c)\tau}d\tau +$$

$$\frac{A_c^2}{4}\int_{-\infty}^{\infty}R(\tau)e^{-j(\omega-\omega_c)\tau}d\tau + \frac{A_c^2}{4}\int_{-\infty}^{\infty}R(\tau)e^{-j(\omega+\omega_c)\tau}d\tau$$

$$= \frac{A_c^2}{4}\delta\left(\omega-\omega_c\right) + \frac{A_c^2}{4}\delta\left(\omega+\omega_c\right) + \frac{A_c^2}{4}\nu\left(\omega-\omega_c\right) + \frac{A_c^2}{4}\nu\left(\omega+\omega_c\right)$$

The result corresponds to the previous conclusions. The signal spectrum is made up of two main portions: the first portion is the pure carrier at ω_c angular frequency, which is represented by the two Dirac delta functions: $\delta(\omega - \omega_c)$ for the positive frequencies, and $\delta(\omega + \omega_c)$ for the negative frequencies.

The second portion is the DSB PSD of the noise signal itself, also mixed to ω_c (see $\nu(\omega - \omega_c)$ and $\nu(\omega + \omega_c)$). It is scaled by $A_c^2/4$, and any absolute measurement of the spectrum incorporates this factor. However, in practice, the measured noise is scaled back in power and shifted back to dc based on the measured carrier to avoid any such dependence. The result is the original noise PSD, $\nu(\omega)$, which is now referred to as the noise PSD relative to carrier.

Next, the phase modulation is examined.

$$c_{PM}(t) = A_c\sin(\omega_c t + n(t))$$
$$= A_c\sin\omega_c t\cos n(t) + A_c\cos\omega_c t\sin n(t)$$

If $n(t) << 1$,

$$\cos(n(t)) \approx 1$$

$$\sin(n(t)) \approx n(t)$$

This allows the expression to be simplified:

$$c_{PM}(t) \approx A_c\sin\omega_c t + n(t)A_c\cos\omega_c t$$

The equations for its PSD can be written as follows:

$$\gamma_{PM}(\omega) \approx \lim_{T\to\infty}\frac{1}{T}\int_{-\frac{T}{2}}^{\frac{T}{2}}\int_{-\frac{T}{2}}^{\frac{T}{2}}E\left[c_{PM}(t_1)c_{PM}(t_2)\right]e^{-j\omega(t_1-t_2)}dt_1dt_2$$

The critical portion is the expected value; it is examined separately.

$$E[c_{PM}(t_1)c_{PM}(t_2)]$$
$$\approx A_c^2E[(\sin\omega_c t_1 + n(t_1)\cos\omega_c t_1)(\sin\omega_c t_2 + n(t_2)\cos\omega_c t_2)]$$
$$= A_c^2E[\sin\omega_c t_1\sin\omega_c t_2 + \sin\omega_c t_1 n(t_2)\cos\omega_c t_2 +$$
$$n(t_1)\cos\omega_c t_1\sin\omega_c t_2 + n(t_1)n(t_2)\cos\omega_c t_1\cos\omega_c t_2]$$
$$= A_c^2\sin\omega_c t_1\sin\omega_c t_2 + A_c^2\cos\omega_c t_1\cos\omega_c t_2E[n(t_1)n(t_2)]$$

The first part is the pure carrier and is the same as in the previous proof; therefore, only the second part is of interest. The t_1 and t_2 variables are replaced with $\tau = t_1 - t_2$ and $\upsilon = t_1 + t_2$, and $E[n(t_1)n(t_2)] = R(\tau)$. The second part is

$$\frac{A_c^2}{2}\left(\cos\omega_c\tau + \cos\omega_c\upsilon\right)R(\tau)$$

Integrated separately for υ variable,

$$\int_{-T+\tau}^{T+\tau}\left(\cos\omega_c\tau + \cos\omega_c\upsilon\right)d\upsilon = 2T\cos\omega_c\tau\left(1+\frac{\sin T\omega_c}{T\omega_c}\right)$$

Substituting this equation back into the PSD calculation,

$$\frac{A_c^2}{2}\lim_{T\to\infty}\left(1+\frac{\sin T\omega_c}{T\omega_c}\right)\int_{-T}^{T}\cos\omega_c\tau R(\tau)e^{-j\omega\tau}d\tau$$
$$= \frac{A_c^2}{2}\int_{-\infty}^{\infty}\cos\omega_c\tau R(\tau)e^{-j\omega\tau}d\tau$$

Finally, putting together all the pieces,

$$\gamma_{PM}(\omega) =$$
$$\frac{A_c^2}{4}\delta\left(\omega-\omega_c\right) + \frac{A_c^2}{4}\delta\left(\omega+\omega_c\right) + \frac{A_c^2}{4}\nu\left(\omega-\omega_c\right) + \frac{A_c^2}{4}\nu\left(\omega+\omega_c\right)$$

Again, it can be seen that the signal spectrum is made up of the pure carrier at ω_c angular frequency, and the DSB PSD of the noise signal itself mixed to ω_c. However, in this case, the mixing is performed by a cosine adding the 90° phase shift.

CONSEQUENCES

Both the deterministic phasor and the stochastic approaches reveal the same far-reaching consequences. First, for low modulation index PM signals, the sidebands are directly connected to the modulation index. Examining the power of the sidebands reveals the power of the phase noise.

Second, any additive noise vector can be interpreted as the sum of AM noise (in phase with the carrier) and PM noise (perpendicular to the carrier). If PM noise is of interest, the AM component must be removed before the phase noise power can be estimated based on sideband powers.

Third, this proof is only valid if the modulation index is low. In any other case, the sideband powers do not have a direct connection with the phase noise power, and estimations based on this conclusion are inherently flawed.

LOW PM MODULATION INDEX CRITERION

The Taylor series of the sine and cosine functions reveal what happens if the modulation index is high. The noise function enters a nonlinear region, which, in case of the simple, deterministic sinusoidal noise, is as follows:

$$\sin\left(A_n \cos\omega_n t\right) = A_n \cos\omega_n t - \frac{A_n^3 \cos^3\omega_n t}{3!} + \frac{A_n^5 \cos^5\omega_n t}{5!} - \cdots$$

The third power, fifth power, and so on in the equation yield harmonics with additional power in the sidebands; the PSD calculation turns into a Bessel's integration. The affiliated equations can be trivially written based on the previously described proofs; however, they are long and provide little insight. Effectively, the sideband power becomes higher than the PM noise power, and the latter cannot be estimated with the former. However, there is no sharp border between low and high modulation index, and it is up to the user to decide if the simple approximations are viable or not.

SIDEBAND POWER

A nonideal clock examined with a spectrum analyzer is not a single, infinitely narrow peak. On the contrary, it has continuous sidebands that fade away into the noise floor without a clear delimitation. The questions to consider are as follows:

1. How much of the sideband power has to be integrated?
2. Is the noise floor part of the sideband power?

The second question can be easily answered: simply compare the noise floor with and without any input signals. The noise of the spectrum analyzer has nothing to do with the clock noise, and therefore it can be disregarded.

The first question requires further discussion. First, the bandwidth of the noise needs to be established. It is tempting to take only the low frequency, high power PSD regions of the signal into account; however, because a wide region is ultimately integrated, the contribution of a very low power, wideband noise can be more than that of the low frequency noise.

Furthermore, because the wideband portion likely originates from thermal noise, it is conceivable that it is white and therefore has infinite energy. Luckily, the combination of parasitic capacitance and equivalent resistance form a low-pass filter (LPF) on most practical circuits, which introduces a roll-off at some point and thus reduces this energy.

To quantify this power, assume that the signal PSD, $\sigma(f)$, is made up of segments of the form $\sigma(f) = \alpha f^{\beta}$ or $\sigma_{dB}(f) = 10\log_{10}\alpha + \beta 10\log_{10}\alpha$. (Note that regular frequency, f, is used here as opposed to the angular frequency, ω; the latter is more applicable to discuss sinusoidal waves, but it is the former that is usually measured.)

Other forms can also be considered, but this form conveniently results in straight lines in the dB vs. decade plots. Using any two points on a segment, its α and β parameters can be calculated. β defines the steepness of the PSD; therefore, if β = −2, the steepness is −20 dB/dec.

$$\beta = \frac{\sigma_{dB}(f_1) - \sigma_{dB}(f_2)}{10\log_{10}\frac{f_1}{f_2}}$$

$$\alpha = \frac{\sigma(f_1)}{f_1^{\beta}}$$

The power under the segments can be calculated with the following integral:

$$P = \int_{f_1}^{f_2} \sigma(f)df = \int_{f_1}^{f_2} \alpha f^{\beta} df = \alpha \int_{f_1}^{f_2} f^{\beta} df$$

$$= \begin{cases} \alpha\left[\frac{f^{\beta+1}}{\beta+1}\right]_{f_1}^{f_2} = \frac{\alpha}{\beta+1}\left(f_2^{\beta+1} - f_1^{\beta+1}\right), & \beta \neq -1 \\ \alpha\left[\ln f\right]_{f_1}^{f_2} = \alpha \ln\frac{f_2}{f_1}, & \beta = -1 \end{cases}$$

Noise with infinite bandwidth (that is, $f_2 = \infty$, as is the case with a simple thermal noise model) can lead to infinite power if $\beta \geq -1$. However, if $\beta < -1$, $f_2^{\beta+1} = 0$, and thus the power is finite and can be calculated:

$$P = -\frac{\alpha}{\beta+1} f_1^{\beta+1}$$

JITTER AND PHASE NOISE

CLOCK

Clock phase noise coupling is examined first with simple mixing (see Figure 6).

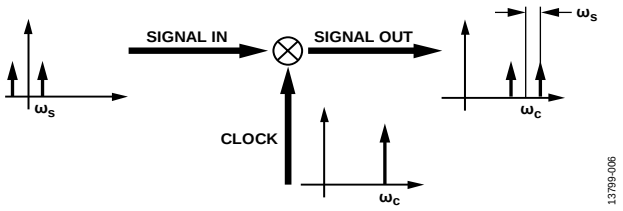

Figure 6. Multiplying a Signal with an Ideal Clock

In this case, multiplying with the clock results in an ideal frequency translation; the signal spectrum is shifted to the clock frequency.

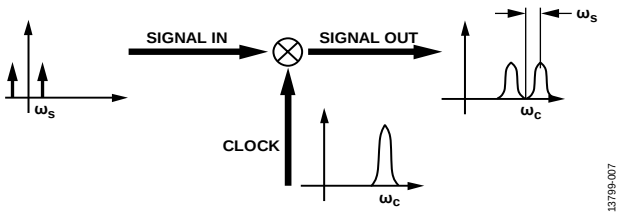

Figure 7. Multiplying a Signal with a Nonideal Clock

A nonideal clock affects the output spectrum (see Figure 7). A multiplication in time domain is equivalent to a convolution in the frequency domain. This phenomenon is called reciprocal mixing, and is of particular importance in the design of radio frequency (RF) transceivers, where an insufficient clock with high phase noise can cause the mixed signal to leak into the adjacent radio channels.

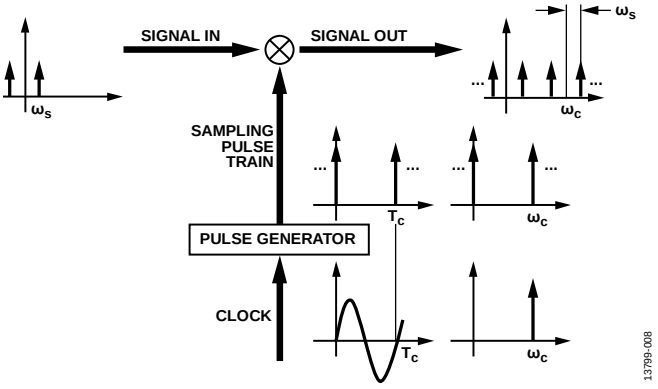

Figure 8. Sampling with an Ideal Pulse Train

However, in case of an ADC sampling clock, neither the ideal nor the nonideal multiplication model can describe precisely the clock noise coupling mechanism and the associated jitter. The simplest sampling model assumes that every rising edge of the clock generates an ideal sampling impulse (see Figure 8, note that both the time and the frequency domain representations of the clock and the sampling pulse train are shown). This pulse train is what is multiplied in time by the input signal to give the sampled output. Note that there is no direct multiplication between the input signal and the clock; therefore, there is no direct convolution between their spectra. It is the spectrum of the sampling pulse train that is convolved with the spectrum of the signal. The spectrum of a pulse train is also a pulse train in the frequency domain, which results in the well known periodic output spectrum as described in the Shannon-Nyquist sampling theorem. The theory proves that if the sampling frequency is high enough, the sampled output signal is an accurate representation of the continuous input signal.

$$s_{OUT}(t) = s_{IN}(t) = A_s \sin\omega_s t$$

where:
$s_{OUT}(t)$ is the output signal.
$s_{IN}(t)$ is the input signal.
A_s is the signal amplitude.
ω_s is the signal angular frequency.

To be perfectly precise, this statement only holds at sampling time points; therefore, lT_c must be employed here instead of t, representing discrete time and continuous time respectively. However, t is used for brevity in most cases.

Using this model, jitter emerges as a natural consequence of clock phase noise.

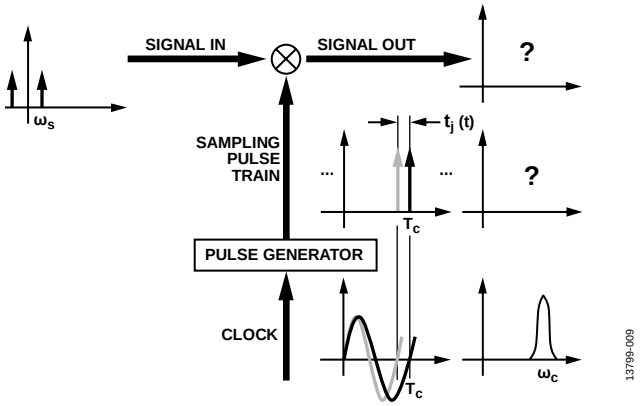

Figure 9. Sampling with a Nonideal Pulse Train

The phase noise moves the sampling pulses in time from their ideal positions (see Figure 9). This deviation from an ideal clock is called time interval error (TIE), $t_j(t)$, which constitutes a good mathematical model but is hard to measure. Instead, the time between consecutive pulses is usually measured to obtain the period or cycle-to-cycle jitter; TIE can then be calculated from period jitter. Note that jitter is fundamentally a discrete time concept: it is only meaningful at sampling times.

The connection between TIE and phase noise is simple. The clock period T_c corresponds to a full circle and an angle of 2π.

$$\frac{t_j(lT_c)}{n(lT_c)} = \frac{T_c}{2\pi}$$

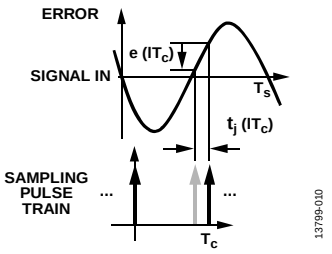

Figure 10. Instantaneous, Additive Error in Time due to Jitter

The modified sampling pulse train has a spectrum that is difficult to express analytically, and so the output spectrum cannot be expressed either. What can be examined instead is the instantaneous, additive error caused by jitter, assuming a sinusoidal input signal (see Figure 10).

$$s_{OUT}(t) = A_s \sin\omega_s(t + t_j(t))$$
$$= A_s \cos\omega_s t_j(t) \sin\omega_s t + A_s \sin\omega_s t_j(t) \cos\omega_s t$$

Note that t is used instead of lT_c only for the sake of brevity.

Assuming that $\omega_s t_j(t) << 1$, the previously discussed approximations can be used.

$$s_{OUT}(t) = A_s \sin\omega_s t + A_s \omega_s t_j(t) \cos\omega_s t$$

Note that $\omega_s t_j(t)$ can be simplified.

$$\omega_s t_j(t) = \omega_s \frac{T_c}{2\pi} n(t) = \frac{\omega_s}{\omega_c} n(t)$$

Therefore, the following simple relationship is obtained:

$$s_{OUT}(t) \approx A_s \sin\omega_s t + A_s \frac{\omega_s}{\omega_c} n(t) \cos\omega_s t = s_{IN}(t) + e_c(t)$$

where $e_c(t)$ is the additive error due to clock jitter.

This result has profound consequences. Given the approximations, the DSB clock phase noise, n(t), is directly mapped around the input signal. The spectrum of the clock signal is directly copied onto the input signal, much like in the case of reciprocal mixing. However, the coupling mechanism is different, and the power is also different due to the $A_s(\omega_s/\omega_c)$ constant.

This result also allows comparisons. Two sampling solutions are equivalent in terms of jitter noise power if

$$\frac{n(t)_1}{\omega_{c1}} = \frac{n(t)_2}{\omega_{c2}}$$

Conversely, if a hypothetical signal generator with frequency-independent, fixed phase noise characteristics is used for the clock, running it at a higher frequency (that is, sampling at a higher rate) reduces the jitter noise power.

ANALOG INPUT

Up to this point, this application note has ignored the fact that the input signal itself needs to be generated, and that process is also nonideal, so the derived results are not fully accurate. However, the tools to describe such a system are now available. The first step is acknowledging that the input signal also has phase noise, m(t). The input and clock phase noises are independent.

$$s_{OUT}(t) = A_s \sin(\omega_s(t + t_j(t)) + m(t + t_j(t)))$$

The $m(t + t_j(t))$ portion can be simplified with a few assumptions. The shape of the signal phase noise is likely a peak in the frequency domain, which is equivalent to a very broad autocorrelation function. In other words, at any given time, the signal phase noise is very similar to previous and future values. Furthermore, $t_j(t) << 1$, so it can be assumed that $m(t + t_j(t)) \approx m(t)$.

$$\begin{aligned} s_{OUT}(t) &\approx A_s \sin(\omega_s(t + t_j(t)) + m(t)) \\ &= A_s \sin\omega_s t(\cos\omega_s t_j(t)\cos m(t) - \sin\omega_s t_j(t)\sin m(t)) + \\ &\quad A_s \cos\omega_s t(\sin\omega_s t_j(t)\cos m(t) + \cos\omega_s t_j(t)\sin m(t)) \\ &\approx A_s \sin\omega_s t(1 - \omega_s t_j(t) m(t)) + \\ &\quad A_s \cos\omega_s t(\omega_s t_j(t) + m(t)) \\ &= A_s \sin\omega_s t - A_s \frac{\omega_s}{\omega_c} n(t) m(t) \sin\omega_s t + \\ &\quad A_s \frac{\omega_s}{\omega_c} n(t) \cos\omega_s t + A_s m(t) \cos\omega_s t \end{aligned}$$

The $A_s \frac{\omega_s}{\omega_c} n(t) m(t) \sin\omega_s t$ portion is likely negligible.

$$\begin{aligned} s_{OUT}(t) &\approx A_s \sin\omega_s t + A_s \frac{\omega_s}{\omega_c} n(t) \cos\omega_s t + A_s m(t) \cos\omega_s t \\ &= s_{IN}(t) + e_c(t) + e_s(t) \end{aligned}$$

where $e_s(t)$ is the additive error due to signal phase noise.

Again, the result shows a surprisingly simple relationship. To take the signal phase noise into account, simply add it.

Finally, the PSD of this signal is examined. The different portions are uncorrelated, and therefore the power can be added up.

$$\sigma_{OUT}(\omega) \approx \sigma_{IN}(\omega) + \varepsilon_c(\omega) + \varepsilon_s(\omega)$$

where:
$\sigma_{OUT}(\omega)$ is the PSD of the output signal.
$\sigma_{IN}(\omega)$ is the PSD of the input signal.
$\varepsilon_c(\omega)$ is the PSD of additive error due to clock jitter.
$\varepsilon_s(\omega)$ is the PSD of additive error due to signal phase noise.

If expanded, the PSD is as follows:

$$\begin{aligned} \sigma_{OUT}(\omega) &\approx \frac{A_s^2}{4}\delta(\omega - \omega_s) + \frac{A_s^2}{4}\delta(\omega + \omega_s) \\ &+ \frac{A_s^2}{4}\frac{\omega_s^2}{\omega_c^2}\nu(\omega - \omega_s) + \frac{A_s^2}{4}\frac{\omega_s^2}{\omega_c^2}\nu(\omega + \omega_s) \\ &+ \frac{A_s^2}{4}\mu(\omega - \omega_s) + \frac{A_s^2}{4}\mu(\omega + \omega_s) \end{aligned}$$

RESULTS RELATIVE TO FULL SCALE

The previous description is mathematically correct, but somewhat cumbersome to use in practical situations, because the absolute signal power, $P_{IN} = A_s^2/2$, is likely not available. The signal generator can be set to a well known value; however, it is not necessarily known what the actual signal level is at the ADC input. Losses, attenuation, reflection, and other variables can affect the signal before it actually arrives at the ADC input. Therefore, instead of an absolute power number in terms of mW, a relative value is used. The input signal power is expressed relative to the power of a sine that results in a full-scale (FS) signal at the input.

$$P_{IN\_FS} = \frac{\frac{A_s^2}{2}}{\frac{A_{FS}^2}{2}} = \frac{A_s^2}{A_{FS}^2}$$

The PSD then becomes,

$$\sigma_{OUT\_FS}(\omega) = \frac{\sigma_{OUT}(\omega)}{\frac{A_{FS}^2}{2}} \approx \frac{P_{IN\_FS}}{2}\delta(\omega - \omega_s) + \frac{P_{IN\_FS}}{2}\delta(\omega + \omega_s)$$
$$+ \frac{P_{IN\_FS}}{2}\frac{\omega_s^2}{\omega_c^2}\nu(\omega - \omega_s) + \frac{P_{IN\_FS}}{2}\frac{\omega_s^2}{\omega_c^2}\nu(\omega + \omega_s)$$
$$+ \frac{P_{IN\_FS}}{2}\mu(\omega - \omega_s) + \frac{P_{IN\_FS}}{2}\mu(\omega + \omega_s)$$

Recall that the signal generator DSB phase noise PSDs, that is $\nu(\omega)$ and $\mu(\omega)$, are not measured in absolute terms, but relative to carrier: the nominal clock signal power for the clock, and the nominal analog input signal power for the analog input.

Finally, the result can be consolidated to positive frequencies only by adding up the power for the negative and positive components.

$$\sigma_{OUT\_FS\_POSITIVE\_\omega}(\omega) \approx$$
$$P_{IN\_FS}\left(\delta(\omega - \omega_s) + \frac{\omega_s^2}{\omega_c^2}\nu(\omega - \omega_s) + \mu(\omega - \omega_s)\right)$$

EXAMPLES

There are deterministic and stochastic subtypes of jitter. The proofs in this application note were kept as nonrestrictive as possible, so that the derived results are generally applicable and can be used to predict signal spectra in various cases.

INTERLEAVED ADC CLOCK SKEW JITTER—APPLYING THE THEORY TO EXPLAIN THE BEHAVIOR OF COMPLEX ADCS

For example, in case of time interleaving converters, multiple identical ADCs process samples at a faster rate than the operating sample rate of each individual converter. The result is an overall higher net sample rate even though each ADC in the array is actually sampling at a lower rate. Therefore, for example, by interleaving four 100 MSPS ADCs, a 400 MSPS ADC can be realized in principle.

However, the concept hinges on individual ADCs having precise and accurate timing. In practice, situations may occur where the clock of one ADC has an offset compared to the others. This offset is commonly referred to as clock skew, which can be interpreted as a deterministic jitter or TIE that repeats to produce a distinctive $t_j(t)$ function. With the theory shown previously, the resulting spectrum can be explained and predicted. The phase noise directly maps onto the output signal as $A_s(\omega_s/\omega_c)$. Therefore, examining the output spectrum is enough to determine if there are any offsets in the timing of interleaved ADCs.

SMA100A SIGNAL GENERATOR AND AD9684 ADC—APPLYING THE THEORY TO PREDICT THE SPECTRUM

In the following example, the Rohde & Schwarz SMA100A signal generator (9 kHz to 3 GHz) was employed as the input clock for a high speed AD9684 ADC. The analog input was supplied by the same type of signal generator. The phase noise measured at 500 MHz is shown in Figure 11.

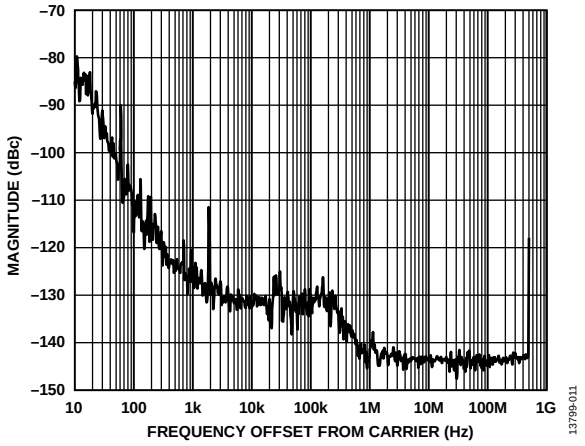

Figure 11. Phase Noise of Rohde & Schwarz SMA100A

With additional input parameters (input frequency of 125 MHz, input power level of −2.0 dBFS, resolution of 14 bits, aperture jitter of 80 fs, input white noise of 1.9 LSB rms, FFT size of 131072), the output spectrum can be estimated (see Figure 12).

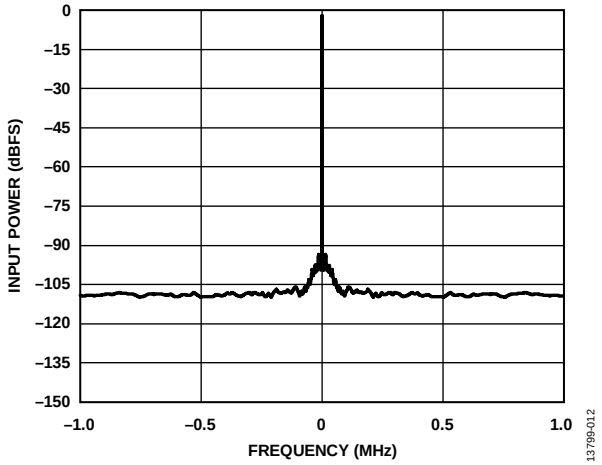

Figure 12. Estimated Output Spectrum

Actual measurement data for this setup is shown in Figure 13. In this case, the mathematical predictions (shown as a thin gray line) correlate very well with the actual measurements. To put this result in perspective, the AD9684 ADC has multistage, pipelined architecture with complicated analog and digital signal processing capabilities, yet its behavior can be predicted using just the simple model shown in Figure 9 and the final equation shown in the Results Relative to Full Scale section.

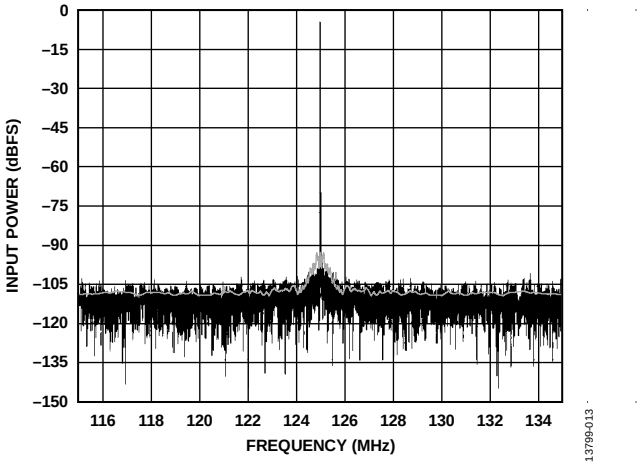

Figure 13. Measured Output Spectrum (with Coherent Sampling)

NOTES

AN13799-0-6/16(0)